Available Online at http://www.journalajst.com

ASIAN JOURNAL OF SCIENCE AND TECHNOLOGY

ISSN: 0976-3376

Asian Journal of Science and Technology
Vol. 16, Issue, 02, pp. 13458-13467, February, 2025

RESEARCH ARTICLE

IDENTIFICATION OF MINING AREAS BY MULTI-CRITERIA ANALYSIS, USING THE POTENTIAL OF RADAR AND OPTICAL IMAGERY IN THE DEPARTMENTS OF ABTOUYOUR AND GUÉRA: CHADIAN CENTRAL MASSIF

Amine Karifene*[1], Podo Mahamat Matar[2], Mackaye Hassan Taïsso[2], Mamadou Malloum Ahmat[1] and Mahamat Ali Ateib[1]

[1]Department of Geomatics, Faculty of Mines and Geology, Polytechnic University of Mongo (Chad)
[2]Department of Geosciences, Faculty of Exact and Applied Sciences, University of Ndjamena (Chad)

ARTICLE INFO

Article History:
Received 27th December, 2024
Received in revised form
17th January, 2025
Accepted 20th January 2025
Published online 22nd February, 2025

Keywords:

Remote sensing; Satellite images; Raster data; Guéra, Alteration, Lineament and Lithology.

ABSTRACT

This work deals with the potential of radar and optical imagery in mapping favorable sites for gold and uranium prospecting in the departments of Abtouyour and Guéra. The objective of this work is to identify potential sites for gold and uranium prospecting. Landsat 9 images, Aster images and Palsar images were used as input data. The lineaments of the study area were extracted from the Palsar images and subsequently validated by geophysical data. The iron oxide index (IOF), clay mineral index (IMA), Relative Band Depth 1, 2 and 3 parameters made it possible to extract hydrothermal alteration minerals and iron oxides. Alteration minerals and iron oxides were extracted by segmentation. Then the lineament density was generated using the lineament file. Favorable sites for gold and uranium prospecting are identified based on a multi-criteria analysis combining the different alteration minerals, iron oxides and lineament density. The results obtained highlight favorable sites located in the far south, far north and central part of the province. Field studies allowed the samples to be collected and analyzed. It was also found that these sites obtained coincide with the artisanal gold mining areas.

Citation: Amine Karifene, Podo Mahamat Matar, Mackaye Hassan Taïsso, Mamadou Malloum Ahmat and Mahamat Ali Ateib, 2025. "Pharmaceuticalsin Drinking Water: Assessing human exposure and Environmental Contamination", *Asian Journal of Science and Technology*, 16, (02), 13458-13467.

INTRODUCTION

Mining plays a crucial role in the economic and industrial development of developing African countries such as Chad. In this context, the identification of potential mining areas is a fundamental step in the planning and implementation of mining projects. The departments of Abtouyour and Guéra, located in the Chadian Massif Central, are of particular interest due to their largely unexplored mineral resources. The use of modern technologies, such as radar and optical imaging, allows for improved mapping and geological assessment of mining areas (Abdelnasser *et al*., 2023), (Sorokoby *et al*., 2010), (Masurkar, 2023), (Mamouch *et al*., 2022). Radar imagery, including synthetic aperture radar (SAR) systems, can provide accurate data on the topography and geological structure of the Earth's surface. On the other hand, optical imaging offers high-resolution images that, when combined with advanced image processing methods, allow the identification of mineralogical indices, the recognition of geological formations and the detection of anomalies characteristic of mineralized zones. Data from optical imaging are essential for assessing the accessibility of mining sites and for planning the necessary infrastructure. By integrating these two technological approaches, it becomes possible to establish a detailed geospatial model of areas potentially rich in mineral resources in the Abtouyour department. This model will not only optimize mining exploration, but also minimize environmental impacts and maximize economic benefits for local communities.

Thus, this study aims to explore the synergistic use of radar and optical imagery for the identification of mining areas in the Abtouyour department, providing valuable tools to decision-makers, investors and researchers for sustainable management of mineral resources in Chad. The results of this research could also serve as a reference for other similar regions in Africa and beyond, thus contributing to more efficient and environmentally friendly mining.

Location of the study area: The departments of Abtouyour and Guéra are located between the 17th degree 50 and the 19th degree of East longitude; and the 11th degree 50 and the 13th degree of North latitude. They are located in the center of the Guéra province which occupies the center of Chad (Figure 1).

Geological framework of the study area: The study area is part of the Sahara metacraton constituting its southern limit (Abdelsalam *et al*., 2002). It is part of the Chadian central massif whose main outcrops are: Aboutelfane, Guéra, Abtouyour and some smaller massifs. This formation of the central massif is the least studied section because of the scarcity of rock outcrops (Diontar *et al*., 2020). These authors emphasize that these rocks were deposited during the collision between the Congo craton and the Sahara metacraton. The study area consists of magmatic, metamorphic and sedimentary rocks. Around Mongo, four groups of rocks are distinguished and placed chronologically (Isseini *et al*., 2013): the first group consists of

dolerites; followed by the second group composed of diorites, granodiorites and hornblende-biotite granites (granite I). The latter is followed by the emplacement of the two-mica granite (granite II) forming the third group. The fourth group concerns the discordant biotite granite. Biotite granites and amphibole granites are also reported around Bitkine in the Abtouyour department (Diontar *et al*., 2020). They also highlighted the presence of doleritic and aplitic dykes. The presence of gabbros-diorites should also be noted. Dating by the U/Pb method made it possible to distinguish (i) ancient granites of a metalliminous to peraluminous, magnesian and alkaline nature (Shellnutt *et al*., 2017). These granites are equivalent to cordilleran-type granites or volcanic arc contexts; (ii) Young granites and rhyolites are peraluminous, ferrous and calc-alkaline and their composition is similar to that of post-collisional granites (high K, calc-alkaline) throughout the metacraton and the central African belt. Their emplacement ages coincide with those of the Ouaddaï massif (Isseini *et al*., 2012), (Pham *et al*., 2017). (Nkouandou *et al*., 2017) studied the Mongo dolerites and showed that their composition ranges from basalt to trachybasalt to basaltic trachyandesite. These dolerites have an affinity with those of Cameroon.

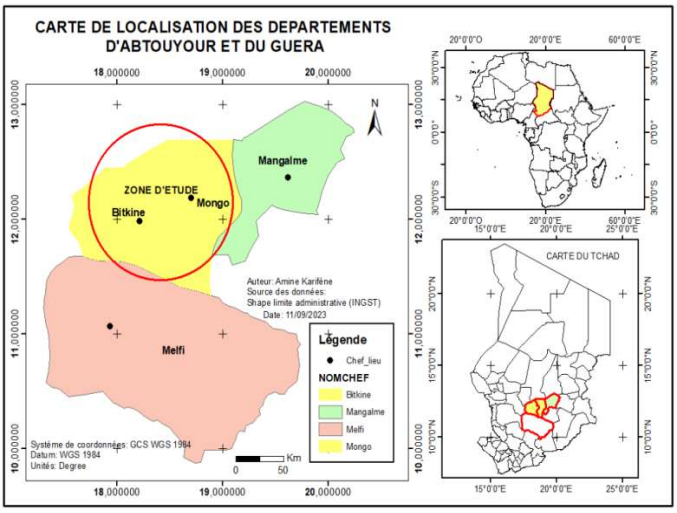

Figure 1. Location of the study area

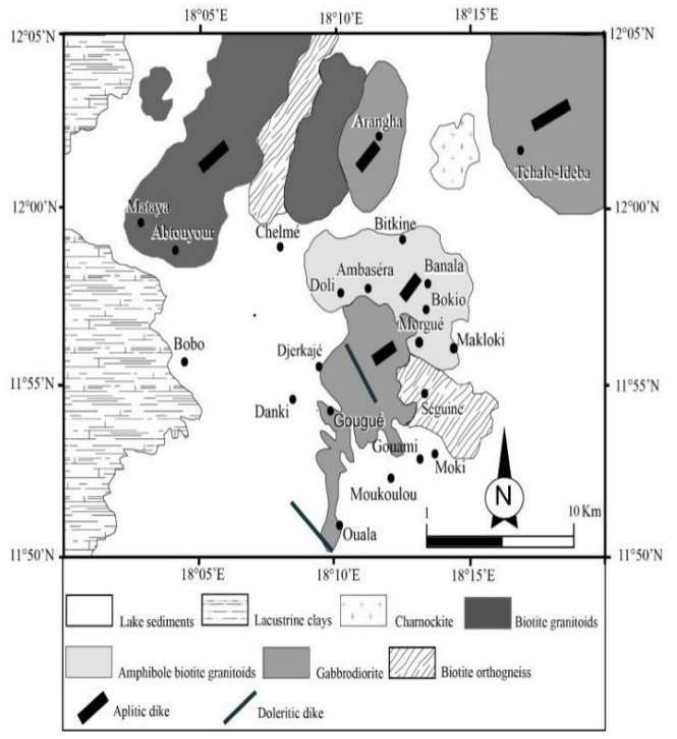

Figure 2. Geological map of the Guéra department (Diontar *et al*., 2020)

MATERIALS AND METHODS

Materials and Data

Materials: As part of this study, materials and data were used to obtain results. A Lenovo core TM i5-13420H brand computer, 2.1 GHz processor, 8G RAM, equipped with a Windows 11 operating system in which software was installed. A Garmin brand GPS was used for collecting data in the field, including identifying points on the ground and recording spatial information. A geologist's hammer and a mass for collecting samples. A compass for measuring the directions and dips of structures. Sample bags to ensure safe transport.

Data and Software

The data used are mainly images: Landsat 9 images, Palsar images and Aster images. Palsar images were used to extract lineaments and define the contours of the formations in the study area. Landsat images were used for lithological and mining mapping. Aster images were used to highlight mining potential. Envi and PCI Geomatica software were used for image processing, Arcgis Pro software for mapping, Rockwork software for determining the major directions of geological structures.

Method: The method adopted in this work is summarized around structural mapping, definition of formation contours, lithological mapping, mapping of hydrothermal alteration minerals and mapping of potential mining sites.

Structural mapping

Preprocessing: This methodology is summarized in: projection of Palsar scenes (to adapt it to the standard projection corresponding to the UTM 34N study area. To completely cover the study area, sixteen (16) Palsar scenes were mosaicked. The delimitation of the study area was done using a vector file in Shape format. As the Radar images contain noise that appears in the image in the form of pepper salt, it is necessary to proceed with the correction in order to eliminate this effect which makes the analysis of the images difficult. The 7X7 window Frost filter was applied to the images for noise reduction. Stretching was then applied to improve the visualization of the images.

Processing: A directional filtering in the four directions (E-W, N-S, NE-SW and NW-SE) was carried out on the resulting image from the preprocessing. Four image files corresponding to the filtering operations in the previous directions are generated and saved in TIFF format. The automatic extraction of the lineaments was done using the PCI Geomatica software thanks to the Line module based on six parameters RADI, GTHR, LTHR, FTHR, ATHR and DTHR. The calibration of these parameters defined according to the values in Table 4.1, made it possible to extract the lineaments which were subsequently exported to the ArcGIS software for their processing and validation. The processing of the Palsar images (correction, mosaicking, filtering) was entirely carried out using the Envi 5.3 and PCI Geomatica software which are very powerful in the processing of Radar and optical images. Figure 3 provides a methodological summary.

Mapping the contours of geological formations: The definition of the contours of the formations was ensured thanks to the corrected and processed Palsar image. These contours will be extracted by digitalization through a visual interpretation of the image. This information is important to know the spatial extent of the different formations present.

Lithological mapping: It was carried out from the ACP principal component analyses and the directed principal component analyses carried out on the OLI2 images. The RGB colored composition of the ratio bands 4/2 6/7 6/5, 6/7 5/6 4/2, 6/7 6/5 4/2 (sabine) also made it possible to efficiently carry out the lithological mapping.

Mapping of hydrothermal alteration minerals: The mapping of alteration minerals was carried out using Aster images by calculating the depth indices of the relative bands (RBD1, RBD2, RBD3 and RBD4). These parameters thus cited made it possible to highlight hydrothermal alteration mineral complexes associated with the mineralization of gold and uranium (Abdelnasser *et al*., 2023), (Abdelkader *et al*., 2022), (Banerjee *et al*., 2019), (Anaba Fotze *et al*., 2022). These indices have proven themselves and have been used in numerous scientific works that have led to satisfactory results. Iron oxide index (IOF), clay mineral index (IMA) parameters were added to the calculation.

Mapping of potential mining sites: The mapping of potential sites for gold and uranium prospecting is carried out through the extraction and superposition of previously obtained information such as mineral complexes from RBD, IMA, IOF and lineament density parameters.

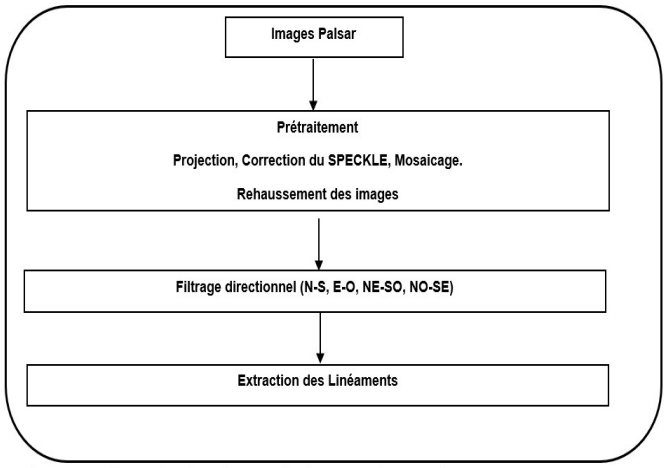

Figure 3. Methodological approach to Palsar image processing

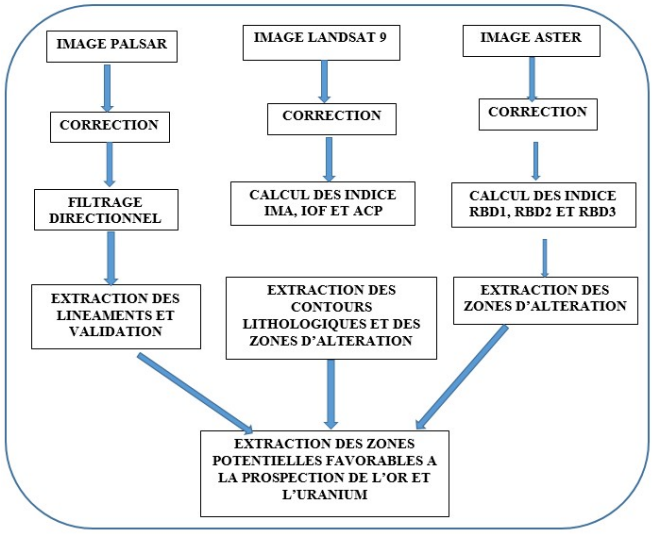

Figure 4. Methodological synthesis

RESULTS

Structural mapping: Figure 4 presents the sixteen (16) Palsar scenes covering the two departments of the study area. These scenes were first mosaicked and then corrected.

Directional filtering in the four directions N-S, E-W, NE-SW and NW-SE was performed on the Palsar images (Figure 5). The images from these four filters were exported to PCI Geomatica software and subjected to lineament extraction. Figure 6 shows the extracted lineaments in the four directions.

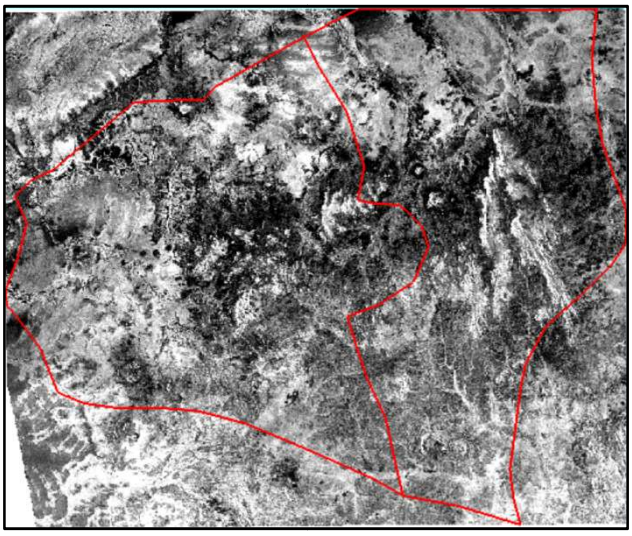

Figure 5. Palsar image of the study area corrected and mosaicked

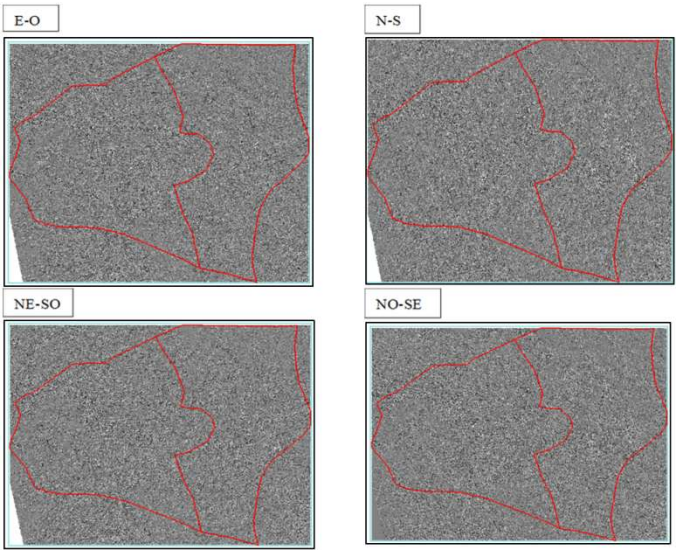

Figure 6. Directional filters (E-W, N-S, NE-SW and NW-SE) from Palsar images

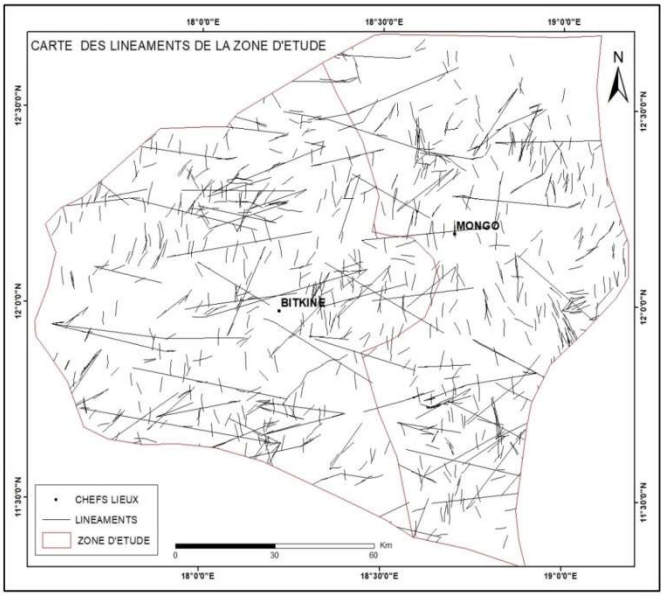

Figure 7. Lineament map from Palsar Radar images

The images from these four filters were exported to the PCI Geomatica software and were subjected to lineament extraction. Figure 6a shows the lineaments extracted in the four directions.

Table 4.1. The E-0 filter operator

-1.000000	-1.000000	-1.000000	-1.000000	-1.000000	-1.000000	-1.000000
-1.000000	-1.000000	-1.000000	-1.000000	-1.000000	-1.000000	-1.000000
-1.000000	-1.000000	-1.000000	-1.000000	-1.000000	-1.000000	-1.000000
0.000000	0.000000	0.000000	0.000000	-0.000000	-0.000000	-0.000000
1.000000	1.000000	1.000000	1.000000	1.000000	1.000000	1.000000
1.000000	1.000000	1.000000	1.000000	1.000000	1.000000	1.000000
1.000000	1.000000	1.000000	1.000000	1.000000	1.000000	1.000000

Table 4.2. The N-S Filter Operator

-1.000000	-1.000000	-1.000000	0.000000	1.000000	1.000000	1.000000
-1.000000	-1.000000	-1.000000	0.000000	1.000000	1.000000	1.000000
-1.000000	-1.000000	-1.000000	0.000000	1.000000	1.000000	1.000000
-1.000000	-1.000000	-1.000000	0.000000	1.000000	1.000000	1.000000
-1.000000	-1.000000	-1.000000	0.000000	1.000000	1.000000	1.000000
-1.000000	-1.000000	-1.000000	0.000000	1.000000	1.000000	1.000000
-1.000000	-1.000000	-1.000000	0.000000	1.000000	1.000000	1.000000

Table 4.3. NE-SO Filter Operator

-1.414214	-1.414214	-1.414214	-0.707107	0.000000	0.000000	0.000000
-1.414214	-1.414214	-1.414214	-0.707107	0.000000	0.000000	0.000000
-1.414214	-1.414214	-1.414214	-0.707107	0.000000	0.000000	0.000000
-0.707107	-0.707107	-0.707107	0.000000	0.707107	0.707107	0.707107
0.000000	0.000000	0.000000	0.707107	1.414214	1.414214	1.414214
0.000000	0.000000	0.000000	0.707107	1.414214	1.414214	1.414214
0.000000	0.000000	0.000000	0.707107	1.414214	1.414214	1.414214

Table 4.4. The NO-SE filter operator

0.000000	0.000000	0.000000	0.707107	1.414214	1.414214	1.414214
0.000000	0.000000	0.000000	0.707107	1.414214	1.414214	1.414214
0.000000	0.000000	0.000000	0.707107	1.414214	1.414214	1.414214
-0.707107	-0.707107	-0.707107	0.000000	0.707107	0.707107	0.707107
-1.414214	-1.414214	-1.414214	-0.707107	-0.000000	-0.000000	-0.000000
-1.414214	-1.414214	-1.414214	-0.707107	-0.000000	-0.000000	-0.000000
-1.414214	-1.414214	-1.414214	-0.707107	-0.000000	-0.000000	-0.000000

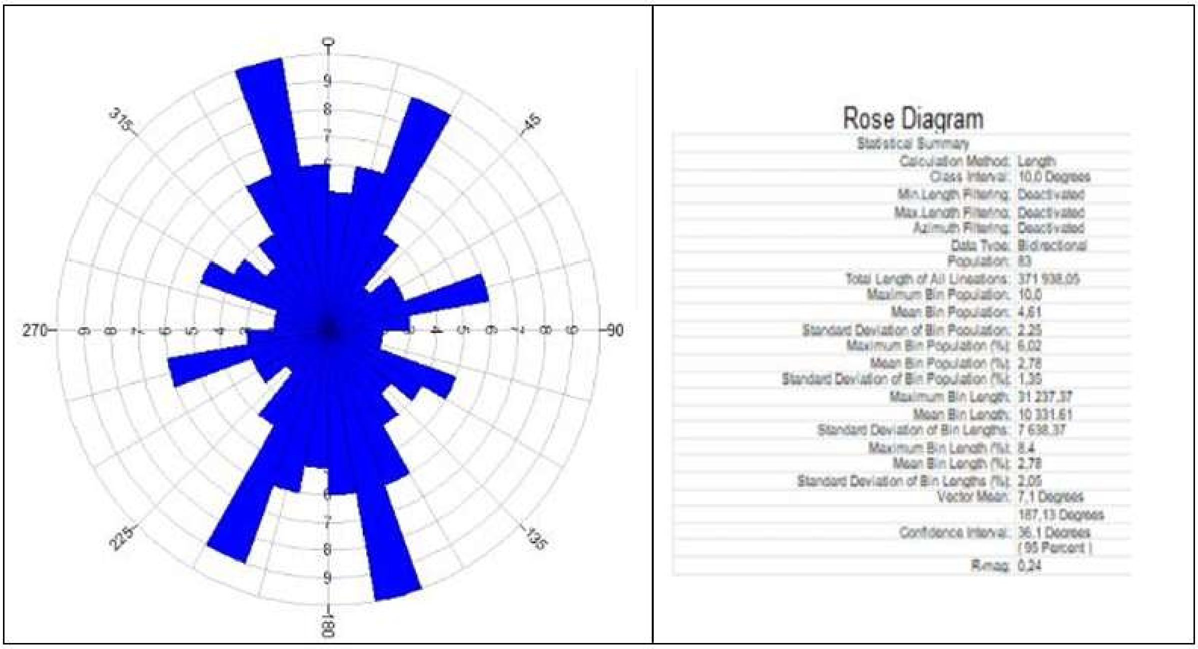

Figure 8. Directional rosette for analyzing major directions

The geophysical data obtained in the study area for the implantation of boreholes in the fracture aquifers made it possible to assess the reliability of the results obtained. As shown in Figure 6b, the different implantations are located either on a lineament or on a intersection of lineaments. The images from these four filters were exported to the PCI Geomatica software and were subjected to lineament extraction. Figure 6a shows the lineaments extracted in the four directions.

The geophysical data obtained in the study area for the implantation of boreholes in the fracture aquifers made it possible to assess the reliability of the results obtained. As shown in Figure 6b, the different implantations are located either on a lineament or on a intersection of lineaments. The principal component analysis performed on the OLI2 images highlighted lithological units in the study area.

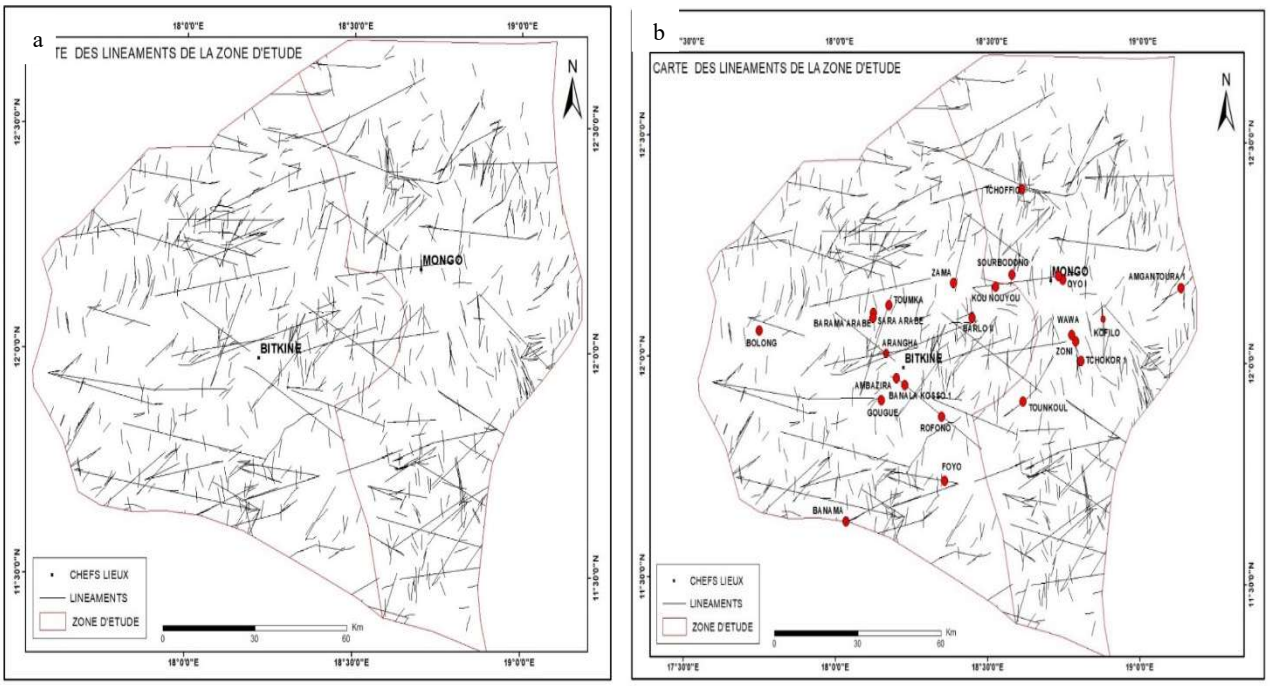

Figure 9. (a) Lineament map, (b) Validation of the Lineament map from Geophysical data

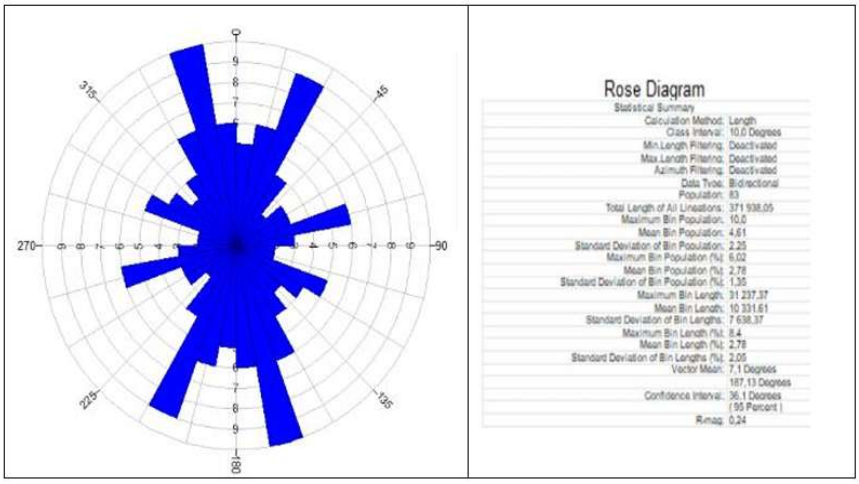

Figure 10. Directional rosette for analyzing major directions

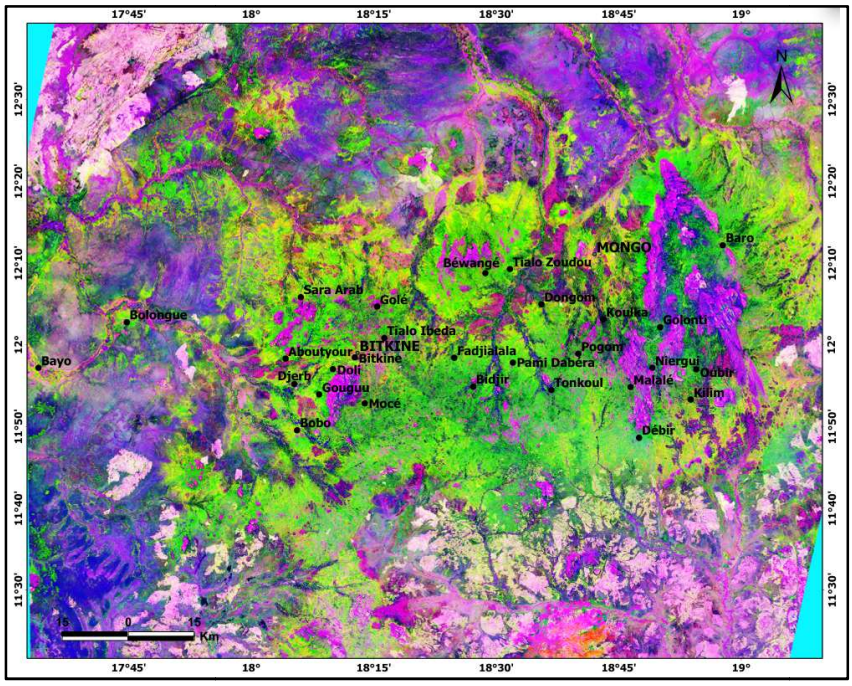

Figure 11. Principal component analysis in RGB (CP1 CP2 CP3)

It made it possible to discriminate the following units: granitoids appearing in bright purple, lateritic curasses in green and sedimentary covers appearing in different colors (dark green, yellowish, dark purple).

Mapping of clay minerals and iron oxides: The calculation of the clay mineral index made it possible to know the distribution of clays expressed on the image by a bright gray tint see figure 9 (IMA). The spatial distribution of iron oxides was highlighted by the calculation of the iron oxide index (IOF) which presents iron oxides in a bright gray tint. (Figure 9 (IOF).

The mapping of clays-hydroxylated minerals and iron oxides, carried out using OLI images from a colored composition of the ratios 4/2, 6/7 and 6/5 respectively placed in the red, green and blue channels, made it possible to highlight the sites rich in iron oxide in pink, the areas rich in clay and hydroxylated minerals (green), the portions dominated by hyperthermal alteration in green-pink or yellow, the ferrous materials are in blue and the granitoids in yellow-green (Figure 10).

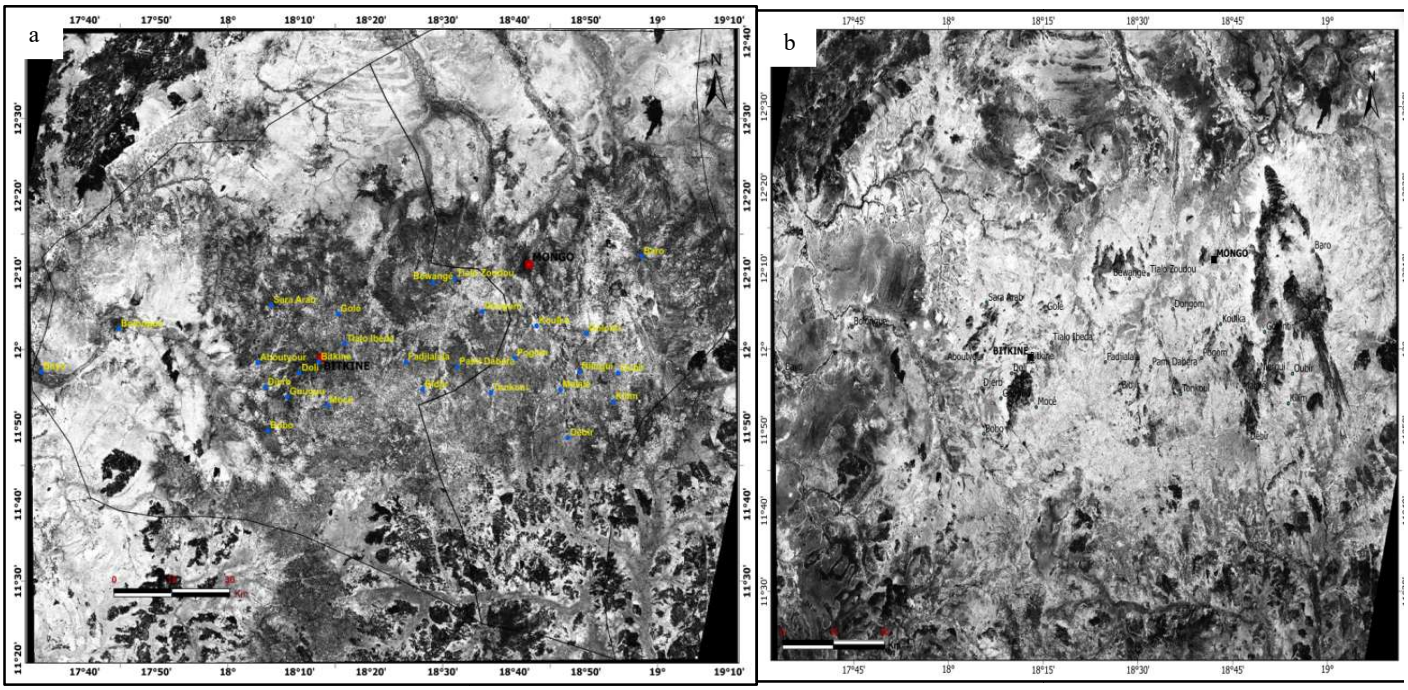

Figure 12. Spatial distribution of clays (a) and iron oxides (b)

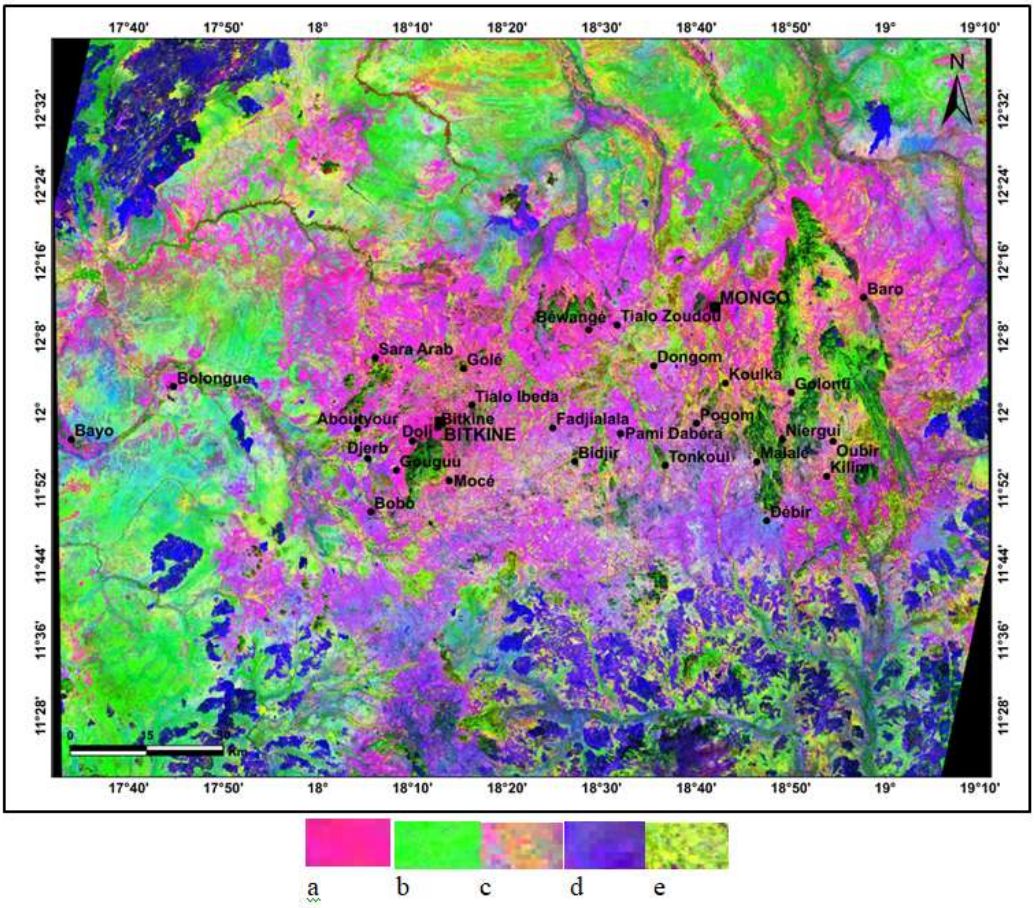

Figure 13. Hydroxyl and oxide minerals on RGB colored composition of ratios 4/2 6/7 6/5 from OLI images

Mapping of the alunite-kaolinite-pyrophyllite mineral group by the Relative Band Depth 1 (RBD1)

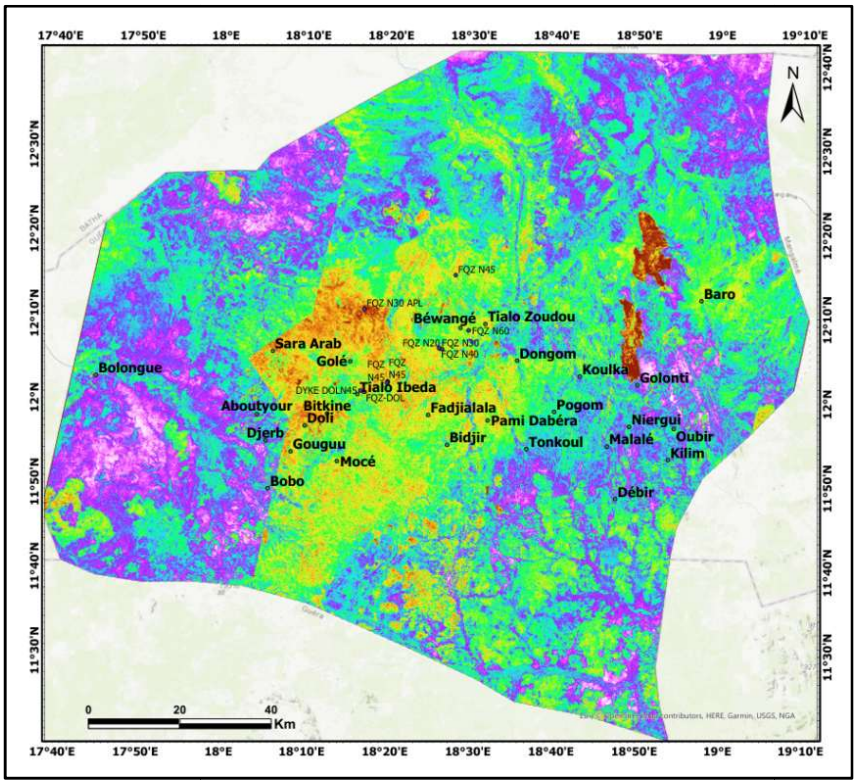

Figure 14. Distribution of the mineral complex alunite-kaolinite-pyrophyllite

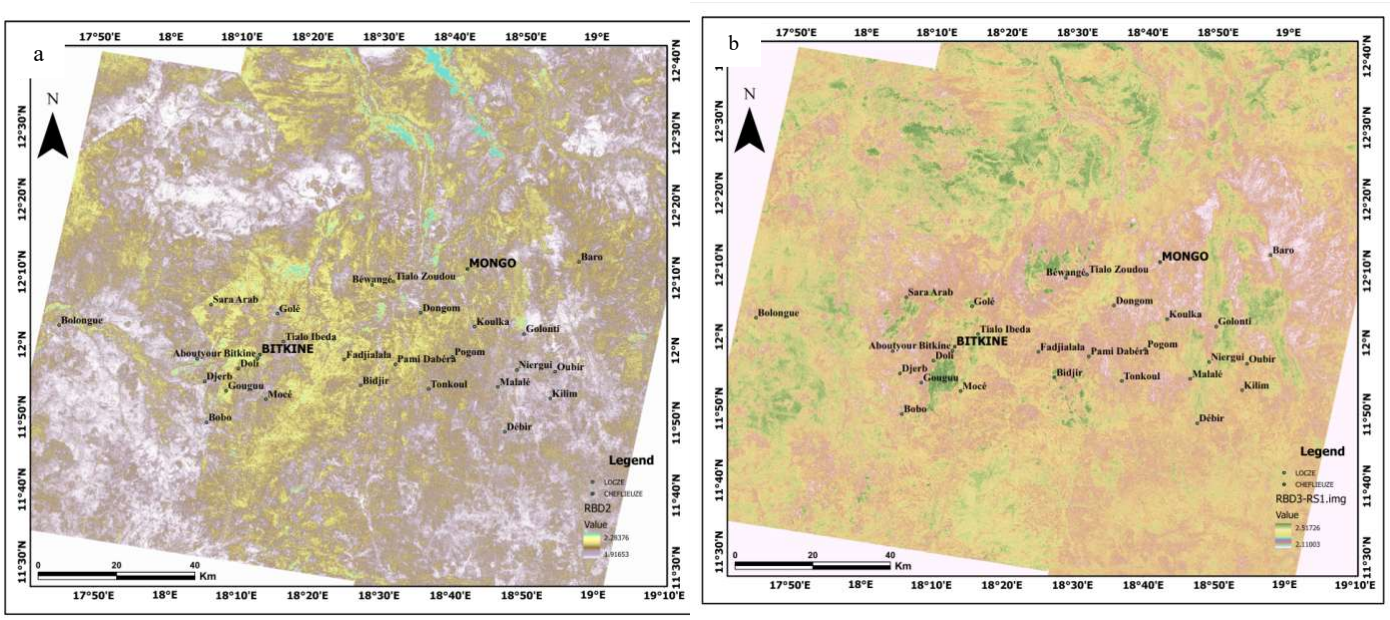

Figure 15. Relative band depth of RBD2 and RBD3 highlighting the sericite-muscovite-illite-smectite mineral complex, appearing yellowish-brown (a) and (b) the chlorite-epidote mineral complex

Mapping of the sericite-muscovite-illite-smectite mineral complex by Relative Band 2 (RBD2) and of the chlorite-epidote mineral complex by Relative Band 3 (RBD3)

RBD2 was used to highlight the sericite-muscovite-illite-smectite minerals, expressed on the imagery of Figure 13a in brown and yellow. In terms of distribution in the study area, this mineral complex is more important than the previous one and is very well expressed in the department of Abtouyour and identified in the localities of Dabakalamar, Tialo-Ideba, Sara-Arabe (Figure 15a).

Figure 13b shows the RBD3 parameter, expressing two chlorite-epidote minerals, appearing in this figure in brown and yellowish. They are identified in the Tiaolo-ideba and Dabakal-amar area. From the previous image, an extraction of the areas corresponding to the mineral group was made. A superposition of all the alteration zones was made to observe the zone of influence of the hydrothermal alteration phenomenon (Figure 16a). Then, the major lineaments were superimposed on the hydrothermal alteration minerals to observe the relationships that exist between them (Figure 16b). This figure shows us that a relationship between the alteration minerals and the lineaments.

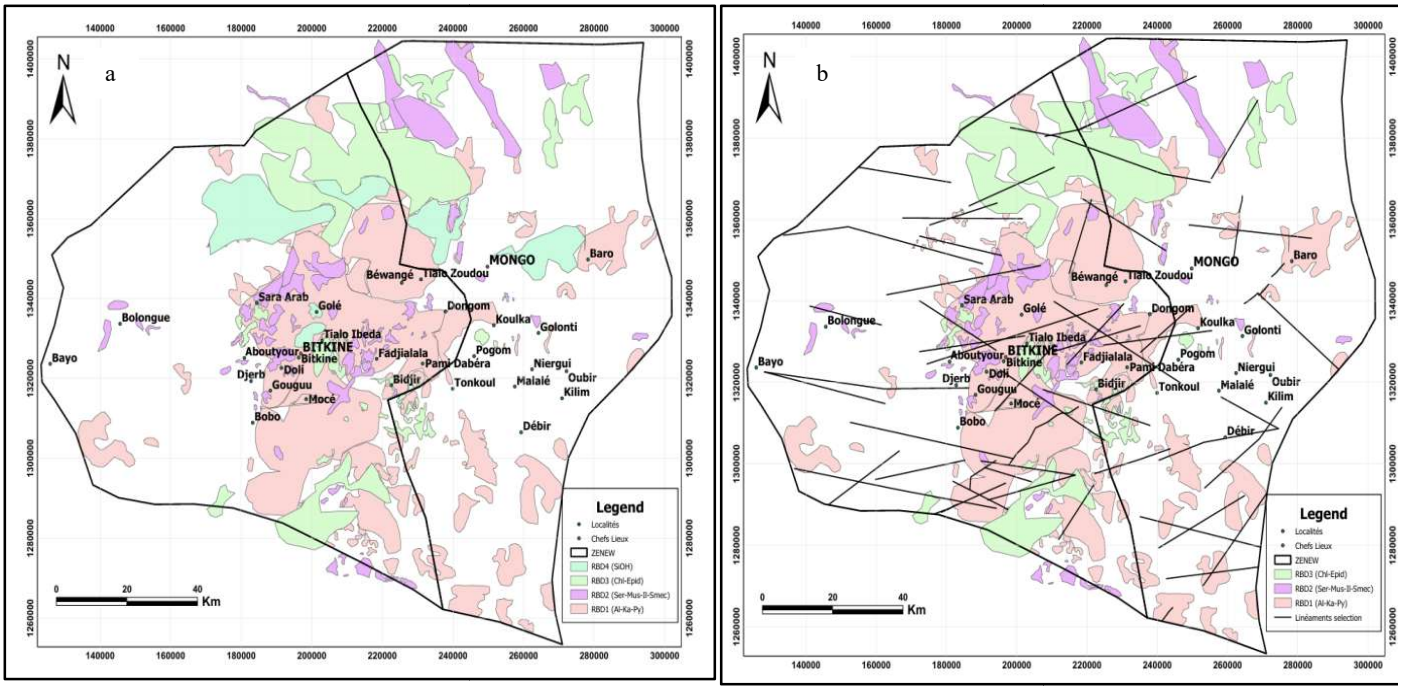

Figure 16. (a) hydrothermal alteration minerals and (b) evidence of the relationship between alteration minerals and major lineaments

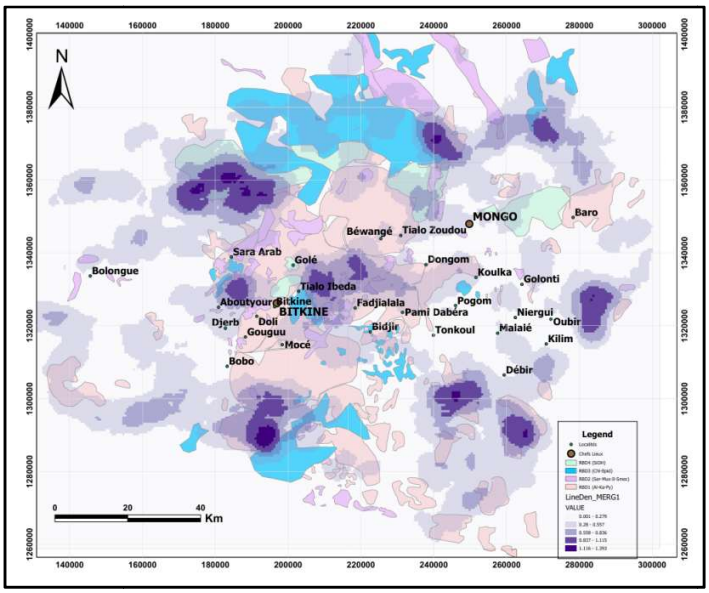

Figure 17. Hydrothermal alteration minerals and lineament density

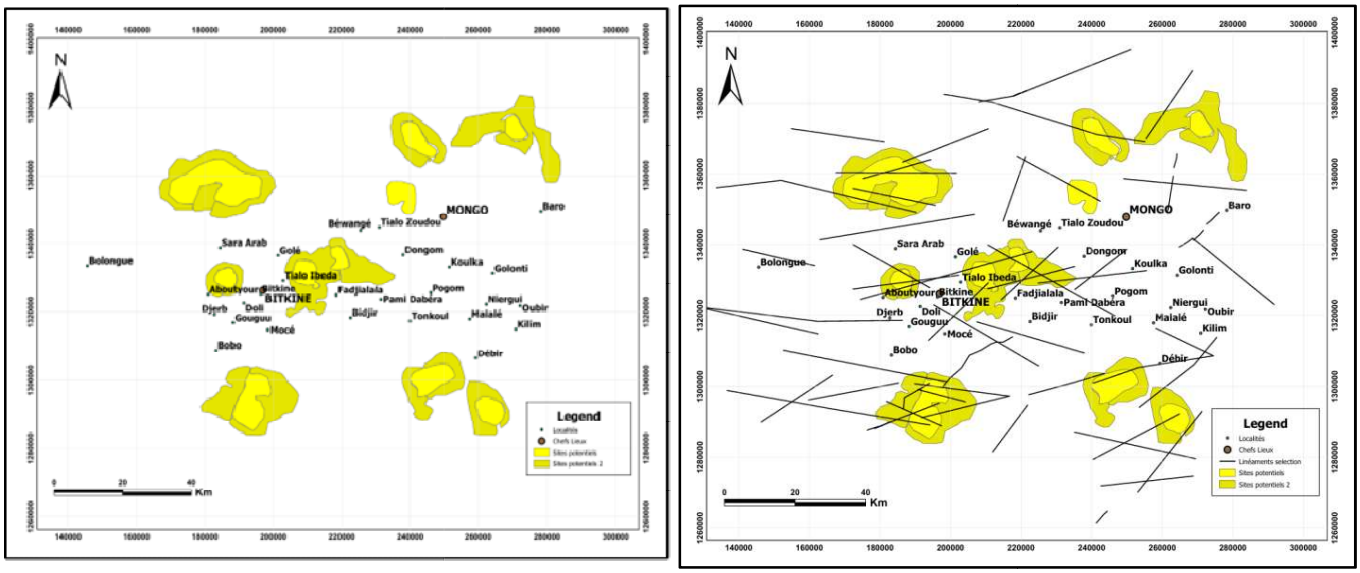

Figure 18. Potential sites suitable for gold and uranium prospecting

Mapping of potential sites favorable to gold and uranium prospecting: To identify sites favorable to gold and uranium prospecting, combinations were made including the nature of the rock, the nature of the hydrothermal alteration mineral and the density of the lineaments. A site is considered potentially favorable when it contains the hydrothermal alteration minerals associated with the mineralization and a high density of lineaments.

A lineament density map was generated using the lineament shape layer as input data (Figure 17). From the combination of the different parameters, the areas favorable to prospecting for gold and uranium were extracted. These areas are classified into high and medium potential zones (Figure 18).

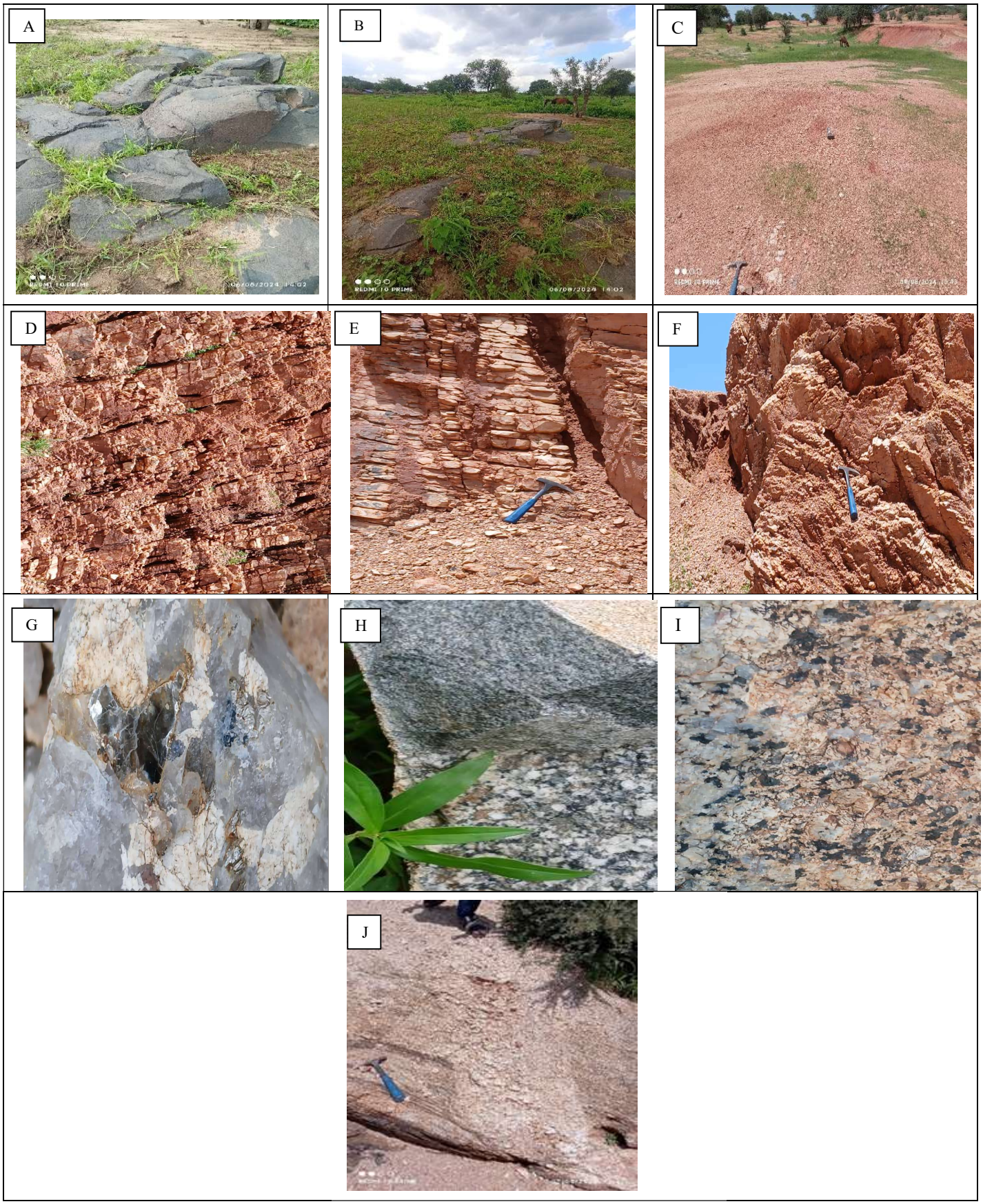

Figure 19. (a) and (b) NE-SW oriented dolerite dyke, (c) quartz vein outcropping in the alteration zone, (d) quartz veinlets alternating with alteration formations, (e) sub-vertical quartz vein intruding the altered zone, (f) quartz vein-altered formation assembly having undergone deformation, (g) quartz vein quartz vein contact with granite, (h) and (i) contact between granular and porphyritic granite, (j) granite intrudet by a NE-SW quartz vein

DISCUSSION OF RESULTS

The selected potential sites that are likely to contain gold and uranium are located in the far north, center and far south of the study area. They are organized into high potential and medium potential sites, classified on the basis of lineament density and alteration mineral expression. Those with a high concentration and strong alteration mineral expression associated with a high lineament density are selected as high potential and so on. The observation is that all alteration minerals are associated with lineaments. So it is important to note that lineaments are associated with mineralization and are the places where fluids responsible for hydrothermal alteration and mineralization deposition circulate. The selected sites were verified by superposition with the mining cadastre database, it emerges from this observation that all sites correspond to the mining areas of the province. 8.

CONCLUSION

Through this work that led us to demonstrate the potential of radar and optical imagery in gold and uranium prospecting, it is interesting to note that Landsat 9, Palsar and Aster images are an important contribution to geology and mining mapping. This work made it possible to map potential sites favorable to gold and uranium prospecting. These sites were verified using field data and the mining cadastre database, and this validation operation shows that these sites correspond well to the gold mining areas of the province.

Acknowledgments: Our thanks to the University of Mongo, which allowed us to carry out this work thanks to its laboratory and its President Professor MACKAYE HASS TAÏSSO for his guidance and availability and to the CDIG (Center for Documentation and Geographic Information) for the data, it provided us and the documentation.

Disclosure of conflict of interest: We affirm on our honor that all the authors who contributed to the writing of this article have no conflict of interest.

REFERENCES

Abdelkader, A., Watanabe, Y., Shebl, A., Hanna, A., A. El-Dokouny, Maher, D., & Csámer, Á. 2022. Efficient delineation of rare metal-bearing granites from remote sensing data using machine learning methods: A case study from the Umm Naggat area, East-Central Desert, Egypt. https://doi.org/10.1016/j.oregeorev. 2022.10518

Abdelnasser, A., Khedr, L., Kharbish, S., Zoheir, B., & Zamzam, S. 2023. Sulfide disseminations and hydrothermal alteration haloes in the Gabal Monqul area, Egypt: Field, mineralogical, and remote sensing studies. *Journal of African Earth Sciences,* 199, 104830.

Abdelsalam, M. G., Liégeois, J.-P., & Stern, R. J. 2002. The saharan metacraton. Journal of African Earth Sciences, 34(3–4), 119–136.

Anaba Fotze, Q. M., Bikoro Bi-Alou, M., Ndougsa-Mbarga, T., Bailly, L., Bernard, J., Penaye, J., Sep Nlomngan, J. P., Djieto Lordon, A. E., Ketchaya, Y. B., & Moussango Ibohn, P. A. 2022. Integrating Aster 07XT, Landsat 8, and aeromagnetic data for the delineation of potential mineralization sites in North Cameroon. *Geological Journal,* 57(9), 3949–3971.

Banerjee, K., Jain, M. K., Jeyaseelan, A., & Panda, S. 2019. Landsat 8 OLI data for identification of hydrothermal alteration zone in Singhbhum Shear Zone using successive band depth difference technique–a new image processing approach. *Current Science,* 116(10), 1639–1647.

Diontar, M., Doumnang, J. C., Kwékam, M., Hamid, Z. A., Dongmo, A. K., Awoum, J. E., & Kouémo, J. T. 2020. Petrogenesis of Magnesian HigH-K Granitoids From Bitkine (Centrechad Massif): Major and Trace Elements Constraints. *European Journal of Environment and Earth Sciences,* 1(5).

Isseini, M., André-Mayer, A.-S., Vanderhaeghe, O., Barbey, P., & Deloule, E. 2012. A-type granites from the Pan-African orogenic belt in south-western Chad constrained using geochemistry, Sr–Nd isotopes and U–Pb geochronology. Lithos, 153, 39–52.

Isseini, M., Hamit, A., & Abderamane, M. 2013. The tectonic and geological framework of the Mongo area, a segment of the Pan-African Guera Massif in Central Chad: Evidences from field observations and remote sensing. *Revue Scientifique Du Tchad,* 1(3), 4–12.

Mamouch, Y., Attou, A., Abdelhalim, M., Mohamed, O., Bouchra, D., Lahsen, A., Yassine, E., Abdelhamid, A., Mustapha, B., Giovanni, R., Stefania, L., & Anselme, M. (2022, January). Mapping of hydrothermal alteration zones in the Kelâat M'Gouna region using airborne gamma-ray spectrometry and remote sensing data: Mining implications (Eastern Anti-Atlas, Morocco). 19.

Masurkar, S. (2023, July). Lineament mapping in the northwestern part of the Gavilgarh fault, Amravati district of Maharashtra using SRTM DEM. *International Journal of Research on Modernization of Engineering Science and Technology*. www.irjmets.com

Nkouandou, O. F., Bardintzeff, J.-M., Mahamat, O., Fagny Mefire, A., & Ganwa, A. A. 2017. The dolerite dike swarm of Mongo, Guéra Massif (Chad, Central Africa): Geological setting, petrography and geochemistry. *Open Geosciences*, 9(1), 138–150.

Pham, N.H.T., Shellnutt, J.G., Yeh, M.-W., & Lee, T.-Y. 2017. A-type granites from the Guéra Massif, Central Chad: Petrology, geochemistry, geochronology, and petrogenesis. 6211.

Shellnutt, J.G., Pham, N.H.T., Denyszyn, S.W., Yeh, M.-W., & Lee, T.-Y. 2017. Timing of collisional and post-collisional Pan-African Orogeny silicic magmatism in south-central Chad. *Precambrian Research*, 301, 113–123.

Sorokoby, V. M., Saley, M. B., Kouamé, F. K., M'Moi, E., Djagoua, V., Bernier, M., Kouadio, A., & Biémi, J. 2010. Use of Landsat ETM+ and SIRS images for linear and thematic mapping of Soubré-Méagui (Southwestern Côte d'Ivoire). REMOTE SENSING, RESEARCH AND APPLICATION REVIEW.

****